The role of Bi and Sb on the electrical properties of Mg doped copper Ferrites

M.A. Ahmed[1], I. K. El Zawawia[2], A. Azab[2] and A.Almuhamady[1]

[1]Materials Science Lab, Physics Department, Faculty of Science, Cairo University, Giza, Egypt
2. National Research Center, Dokki, Giza, Egypt
a.almuhamady@yahoo.com

Abstract: A series of $Cu_{0.7}Mg_{0.3}M_yFe_{2-y}O_4$ spinel ferrites with M = Bi, Sb and $0.0 \le y \le 0.25$, have been prepared by standard ceramic technique. X-ray diffraction (XRD) studies revealed a single phase spinel structure with small secondary phase at some concentrations. Lattice parameter and X-ray density were calculated and reported. Seebeck coefficient was measured, their values for all samples were positive, indicate the majority of charge carriers were holes (p-type). ac conductivity and dielectric constant as a function frequency and temperature were carried out. The measured transport properties were decreased with increasing of Sb^{3+} while increased with Bi^{3+} content up to y=0.15 and then decreased again. .
[M.A. Ahmed, I. K. El Zawawia, A. Azab and A. Almuhamady. **The role of Bi and Sb on the electrical properties of Mg doped copper Ferrites.** *J Am Sci* 2012;8(7):560-574]. (ISSN: 1545-1003). http://www.jofamericanscience.org. 87

Key words: Cu-ferrite, dielectric, conductivity, Bi and Sb

1. Introduction

Spinel ferrites having the general formula AB_2O_4 are very promising materials for many technological applications. Spinel type ferrites are commonly used in many electronic and magnetic devices due to their high magnetic permeability and low losses [1, 2], also they can be used in electrode materials at high temperature applications because of their high thermodynamic stability, electrical conductivity, electrocatalytic activity and resistance to corrosion [3,4]. Mixed copper ferrites have been commonly used for many years in high frequency devices such as radio frequency coils, transformer cores, rod antennas and magnetic cores of read-write heads for high speed digital tapes [5, 6]. In the present work, we have decided to study, the effects of Sb and Bi substitutions on the electrical properties of Cu –Mg ferrites. Another goal was to study the characterization due to substitution of different elements with different ionic radii.

2. Experimental techniques

The samples under investigation were prepared by standard ceramic technique, where high purity oxides were mixed together in stoichiometric ratio according to the formula $Cu_{0.7}Mg_{0.3}M_yFe_{2-y}O_4$, where M = Bi, Sb and $0.0 \le y \le 0.25$. The mixed oxides were grinded manually in agate mortar for 3 hrs and compressed to pellet form using uniaxial hydraulic press with pressure of $1.96x10^8$ N/m^2. The pellets were pre-sintered at 850 ^oC for 6 hrs with heating rate of 4^{o}C/min. using Lenton furnace UAF 16/15(UK). The samples were grinded again and then pressed into pellets and finally sintered at 1100°C for 6 hrs using the same rate and cooled to room temperature with the same rate as that of heating. The pellets were good polished and covered with silver past and checked for good conduction.

The structural properties of $Cu_{0.7}Mg_{0.3}M_yFe_{2-y}O_4$, were investigated by X-ray diffraction (XRD) (Proker D8) with Cu Kα radiation of wavelength λ = 1.5481 Å. The ac conductivity and dielectric properties measurements as a function of frequency (100 kHz – 5 MHz) were performed at different temperatures using RLC bridge model HIOKI 3531 (Japan). The temperature of sample was measured using T-type thermocouple with junction just in contact with the sample to avoid temperature gradient, the accuracy of measuring temperature was ± 1 ^{0}C. The thermoelectric power measurements (Seebeck coefficient) were carried out to determine the type of charge carriers.

3. Results and Discussion

3.1 Structure

Figure (1) shows the X-ray diffraction patterns for $Cu_{0.7}Mg_{0.3}Sb_yFe_{2-y}O_4$ where $0 \le y \le 0.25$. The samples showed cubic spinel structure with small intensity of $FeSb_2O_6$ at (y=0.15 and y=0.25) and another phase of $CuFeO_2$ appeared at (y=0.25). Table (1) reported the variation of the lattice parameter and X-ray density (D_X) with Sb^{3+}contents. It can be seen from the data that the lattice parameter increases from y=0 to y=0.05 which is acceptable result because the ionic radius of Sb^{3+} (0.76 Å) [7] is greater than of Fe^{3+} (0.64 Å) [7] , at y>0.05 the lattice parameter is very slightly decreased, due to the small secondary phase appeared which resides on the grain boundaries of the spinel lattice. This will cause a mismatch between grain and grain boundaries due to the difference in thermal expansion of both phases. The fruitful result is the decrease of the crystallite size with increasing Sb^{3+} content. This was ascribed to the microstrain on the octahedral sites due to the

presence of Sb^{3+} on the expense of Fe^{3+} ions. From table (1) we note that the X-ray density increases with increasing Sb^{3+} content, also we note that, the crystal size decreases with increasing Sb^{3+} content.

Figure (2) shows the X-ray diffraction patterns for $Cu_{0.7}Mg_{0.3}Bi_zFe_{2-z}O_4$; $0 \le z \le 0.25$, The X-ray chart showed the existence of a single phase cubic spinel ferrites without any extra lines corresponding to any other phases. The data in table (2) show the variation of lattice parameter and D_x with Bi^{3+} contents. It is clear that the lattice parameter increases from z=0 to z=0.05. This was an acceptable result because Bi^{3+} has large ionic radius (1.03 Å) [7] compared with Fe^{3+} ions (0.64 Å) [7]. With increasing Bi^{3+} content from z=0.05 up to z=0.25, the lattice parameter decreases. Here Bi^{3+} behaves as a rare earth ion, so one could expect that two diffusion mechanisms can be occurred, the first one is the surface diffusion and the second is the volume diffusion. In our case, volume diffusion is the most probable and this is clear from XRD where no secondary phases appeared. Another explanation of this trend is the low melting point of Bi (630 ^{o}C) therefore a high reactivity and partial incorporation into the spinel lattice takes place, which is a similar trend to the rare earth R^{3+} doping which impedes the grain growth and prevents the existence of inner pores which enhances the densification as well as the decrease in crystal size. The increase of D_x with Bi^{3+} contents assures our suggestion.

3.2 Seebeck Coefficient:

Figure (3) shows the Seebeck coefficient with the average of absolute temperature for the samples ($Cu_{0.7}Mg_{0.3}Sb_yFe_{2-y}O_4$; $0.05 \le y \le 0.25$). The data in the figure show that the Seebeck coefficient is positive for all samples except y=0.10, which is positive from 300 up to 345K after that it becomes negative. These positive values of Seebeck coefficient indicate that the majority of charge carriers are holes. The increase in Seebeck coefficient with temperature indicates that the conductivity is due to thermally activated mobility not to thermally creation of more charge carriers.

Figure (4) shows the dependence of Seebeck coefficient on average of absolute temperature for the third group ($Cu_{0.7}Mg_{0.3}Bi_zFe_{2-z}O_4$; $0.05 \le z \le 0.25$). The Seebeck coefficient is positive for all samples indicating that the predominant conduction mechanism of this group is p-type. The values of Seebeck coefficient increased with temperature up to certain temperature beyond it, the value decreases with increasing temperature [8-11]. The positive value of Seebeck coefficient increases with increasing Bi^{3+} content up to z=0.15 then decreases. This is due to the increase of Bi^{3+} ion content which decreases the number of available of Fe^{3+} ions on the B-site. Thereby decreasing the ratio of Fe^{3+}/Fe^{2+} leading to a decrease in the hopping probability and/or the number of hopping e^{-}.

3.3 dc Conductivity

Figure (5) shows the dependence of dc conductivity $\ln\sigma$ as a represntive curve on the reciprocal of absolute temperature for the samples of ($Cu_{0.7}Mg_{0.3}M_yFe_{2-y}O_4$; where M=Sb and Bi:$0.05 \le y \le 0.25$). The data clarify that the dc conductivity exhibits a semiconducting behavior where it increases with increasing the temperature up to certain value called T at which a change of slope has been occurred, the transition temperatures T are reported in tables (3, 4) Comparing the values of T of the investigated samples with the Curie point reported in table (3, 4) for the same composition one can find that T values agree well with the reported Curie temperatures. Therefore, this transition T is due to the magnetic transition from ferromagnetic ordering to paramagnetic ordering. It is clear that the transition temperatures decreases with increasing Sb^{3} and Bi^{3+}ions content. The activation energies, E_I; E_{II} at low and high temperature regions respectively for all samples were calculated and reported also in table(3, 4), from which the data of the activation energy increases with increases Sb^{3+} ion, where increasing Sb^{3+} ions decrease the amount of Fe^{3+} in octahedral site thereby reduces the hopping conduction between Fe^{3+} and Fe^{2+} then increasing the activation energy, as well as the resistivity. In table (4), it is clear that the activation energy decreases with increasing Bi^{3+} content up to z=0.15 and then increases which indicate the resistivity decreases with Bi^{3+} content up to z =0.15 and then increases.

3.4 ac Conductivity

Figure (6) shows representive curve of $\ln\sigma$ (Ω^{-1} cm^{-1})versus $1000/T(K^{-1})$ for ($Cu_{0.7}$ $Mg_{0.3}$ M_y $Fe_{2-y}O_4$; $0.05 \le y \le 0.25$ M=Sb and Bi) in the frequency range (10kHz– 5 MHz). The figure shows that σ exhibits a semiconducting like behavior with the temperature, where the ac conductivity increases with increasing the temperature, due to increase in the drift mobility of the thermally activated charge carriers according to the hopping conduction mechanism. More than one straight lines with

different slopes are obtained indicating different conduction mechanism. In ferrite samples such as those under investigation the most probable conduction mechanism is the small polaron mechanism rather than the classical barrier hopping mechanism [12]. The conductivity increases with frequency up to certain value where the frequency acts as a pumping force pushing the localized charges between the different conduction states. The data from tables (3, 4) shows that the activation energy at low temperature region (E_I) is lower than that at higher temperature region (E_{II}), which was expected because by increasing temperature up to certain limit the thermal agitation increases and the scattering of charge carriers takes places as the result of the interaction between charges and phonons was also increased.

3.5 Dielectric properties

The mechanism of polarization in polycrystalline ferrites is mainly reported to be hopping of electrons between ions of the same element but with different oxidation states [13]. As the electrons reach the grain boundary on application of an electric field, they pile up and a charge build up takes place, causing interfacial polarization. This type of polarization affected by many factors such as sintering temperature, structural homogeneity, stoichiometry, density, grain size and porosity. Higher density sample implies decreased porosity and higher number of polarizing species per unit volume, both contributing to the observed increase in polarization. The effect of frequency on the ac electrical conductivity σ_{ac}, $\varepsilon^{/}$ and tanδ was theoretically studied [14-16]. The simplest expression indicates that σ_{ac} is directly proportional to the angular frequency ω while $\varepsilon^{/}$ and tanδ are inversely proportional to ω as follows [17]:

$$\varepsilon^{\backslash} = 4\pi\, \sigma_{ac} / (\omega\ \tan\delta) \quad (1)$$

The real $\varepsilon^{/}$ and imaginary $\varepsilon^{//}$ parts of the dielectric constant and the loss tanσ are given by the following Debye equations [18]:

$$\varepsilon^{\backslash\backslash} = \frac{(\varepsilon_s - \varepsilon_\infty)\omega\tau}{1+\omega^2\tau^2} \quad (2)$$

$$\tan\delta = \frac{\varepsilon^{\backslash\backslash}}{\varepsilon^{\backslash}} = \frac{\sigma_{AC}}{\omega\varepsilon^{\backslash}} = \frac{(\varepsilon_s - \varepsilon_\infty)\omega\tau}{(\varepsilon_s + \varepsilon_\infty\omega^2\tau^2)} \quad (3)$$

$$\tan\delta = \frac{\varepsilon^{\backslash\backslash}}{\varepsilon^{\backslash}} = \frac{\sigma_{AC}}{\omega\varepsilon^{\backslash}} = \frac{(\varepsilon_s - \varepsilon_\infty)\omega\tau}{(\varepsilon_s + \varepsilon_\infty\omega^2\tau^2)} \quad (4)$$

wheree τ, ε_s and ε_∞ are relaxation time, dielectric constant at very low and at very high frequency, respectively. Eqs. (2-4) indicate that $\varepsilon^{/}$, $\varepsilon^{//}$ and tanδ decrease as the frequency increases.

Figure (7) correlate the real part of the dielectric constant ($\varepsilon^{/}$) versus T(K) for ($Cu_{0.7}Mg_{0.3}Sb_yFe_{2-y}O_4$ $0.05\leq y\leq 0.25$) in the frequency range (100kHz – 5MHz). The real part of dielectric constant increase very slowly at low temperature region and after which it increases suddenly due to orientation of more free dipoles in the field direction. The sample with y=0.15 shows peak at T=635 K, this peak positions and peak values decrease with increasing frequency. The sample y=0.25 show peak at low temperature region T=345 K. When comparing X-ray charts for Sb contents one can find that, a secondary phase begins to appear at y =0.15 but with small intensity as $FeSb_2O_6$. At y=0.25 the secondary phase appears with more intensity peaks as of $FeSb_2O_6$. The appearance of a hump in dielectric constant at (y=0.25) is due to such secondary phase because help in accumulation of space charge on the grain boundaries, causes an increase in the polarization as well as $\varepsilon^{/}$. Fig.(8) shows the variation of ($\varepsilon^{/}$) with temperature for ($Cu_{0.7}Mg_{0.3}Bi_zFe_{2-z}O_4$ $0.05\leq z\leq 0.25$) in the frequency range (10kHz – 5MHz). A nearly same trend as that in case of Sb was obtained.

Figure (9) correlates loss factor ($\varepsilon^{//}$) versus T(K) as function of applied frequency (100kHz-5MHz) for ($Cu_{0.7}Mg_{0.3}M_yFe_{2-y}O_4$; M=Sb and Bi: $0.05 \leq y\leq 0.25$). at different temperature up to 700K. The loss factor ($\varepsilon^{//}$) increase with temperature up to maximum value then decreases and then increases.

3.6 Composition dependence

The effect of Sb^{3+} ion substitution on ac conductivity (lnσ), ($\varepsilon^{/}$) and ($\varepsilon^{//}$) for ($Cu_{0.7}Mg_{0.3}Sb_yFe_{2-y}O_4$ $0.05\leq y\leq 0.25$)is represented in Fig.(10) at room temperature and at 1 kHz. It is observed that ln $^{/}$ and $^{//}$ decrease as Sb^{3+} ion substitution increases. This is acceptable result where by increasing Sb^{3+} ions the amount of Fe^{3+} in octahedral site will be decreased which in turns reduces the hopping conduction between Fe^{3+} and Fe^{2+}. This will increase the resistivity and decreasing , lnσ , $\varepsilon^{/}$ and $\varepsilon^{//}$.

The effect of Bi^{3+} ion substitution on ac conductivity lnσ, $\varepsilon^{/}$ and $\varepsilon^{//}$ for ($Cu_{0.7}Mg_{0.3}Bi_zFe_{2-z}O_4$ $0.05 \leq z\leq 0.25$) is represented in Fig.(11) at room temperature and 1 kHz. It is observed that lnσ,$\varepsilon^{/}$ and $\varepsilon^{//}$ increase up to z=0.15 then decrease. As previously reported here the positive Seebeck coefficient increases with Bi^{3+} ion content up to z=0.15 then decreases which increase the conductivity up to the same concentration (z=0.15). The composition

dependence of lattice parameter table (2) it decreases with increasing Bi^{3+} ion then decreases, the inter ionic distance between the ions (Fe^{2+} and Fe^{3+}) decrease, the conductivity increases.

Table (1). Lattice parameter (*a*), X ray density (D_X) and particle size for $Cu_{0.7}Mg_{0.3}Sb_yFe_{2-y}O_4$; $0.05 \le y \le 0.25$

Sample	Lattice parameter (*a*) Å	Dx (g/cm^3)	Crystal size (nm)
y=0	8.372	5.151	127.8
y=0.05	8.408	5.159	100.0
y=0.15	8.407	5.309	86.0
y=0.25	8.403	5.464	48.0

Table (2). Lattice parameter (*a*), X ray density (D_X) and particle size for $Cu_{0.7}Mg_{0.3}Bi_zFe_{2-z}O_4$; $0.05 \le z \le 0.25$

Sample	Lattice paramter (*a*) Å	Dx (g/cm^3)	Crystal size (nm)
z=0	8.372	5.151	127.8
z=0.05	8.392	5.287	82.6
z=0.15	8.380	5.655	129.0
z=0.25	8.368	6.026	76.0

Table (3) The values of Curie temperatures, the transition temperatures T_σ ; the activation energies for conduction E_I and E_{II} for $Cu_{0.7}Mg_{0.3}Sb_yFe_{2-y}O_4$;$0.05 \le y \le 0.25$

y	T_C(K)	Transtion temperature		Activation energy (eV)	
		T_{dc}(K)	T_{ac}(K)	E_I	E_{II}
0.05	626	520	623	0.28	0.56
0.10	604	603	606	0.28	0.60
0.15	588	590	588	0.34	0.73
0.20	582	573	572	0.46	0.82
0.25	575	570	568	0.50	0.90

Table (4) The values of Curie temperatures, the transition temperatures T_σ ; the activation energies for conduction E_I and E_{II} for $Cu_{0.7}Mg_{0.3}Bi_zFe_{2-z}O_4$; $0.05 \le z \le 0.25$

z	T_C(K)	Transtion temperature		Activation energy (eV)	
		T_{dc}(K)	T_{ac}(K)	E_I	E_{II}
0.05	630	625	628	0.286	0.788
0.10	640	625	625	0.215	0.506
0.15	628	622	623	0.201	0.408
0.20	618	620	620	0.240	0.716
0.25	610	604	606	0.286	0.752

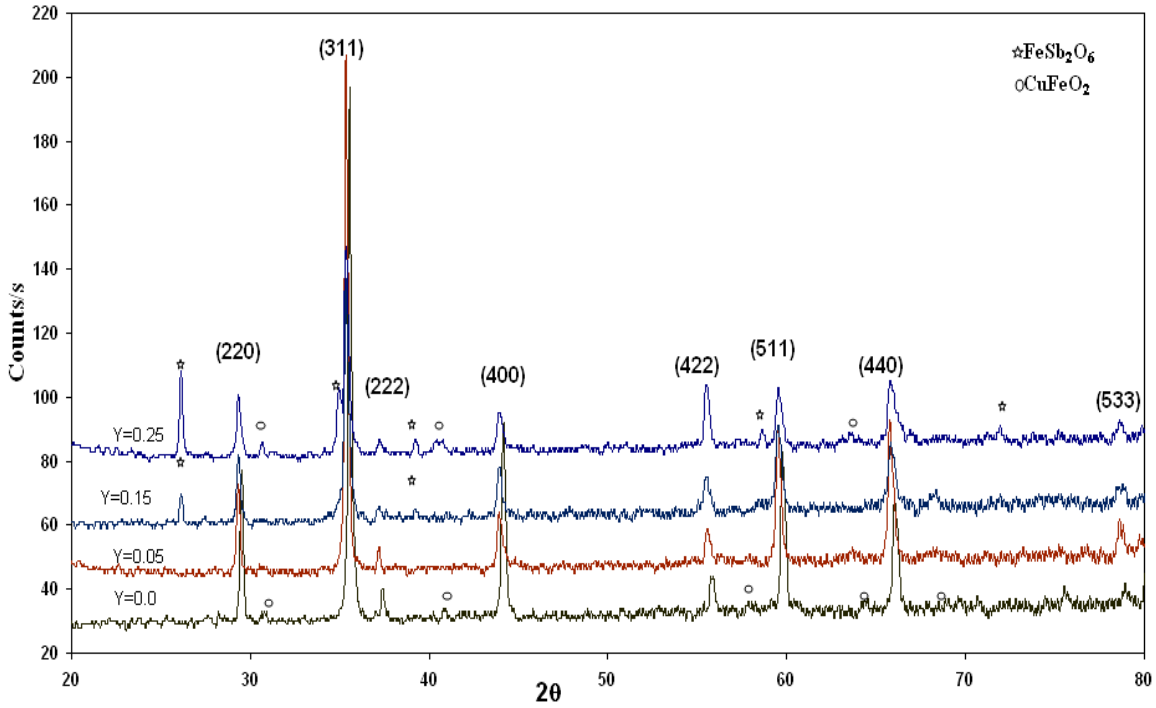

Fig.(1) X-ray diffraction pattern of $Cu_{0.7}Mg_{0.3}Sb_yFe_{2-y}O_4$; $0.0 \leq y \leq 0.25$

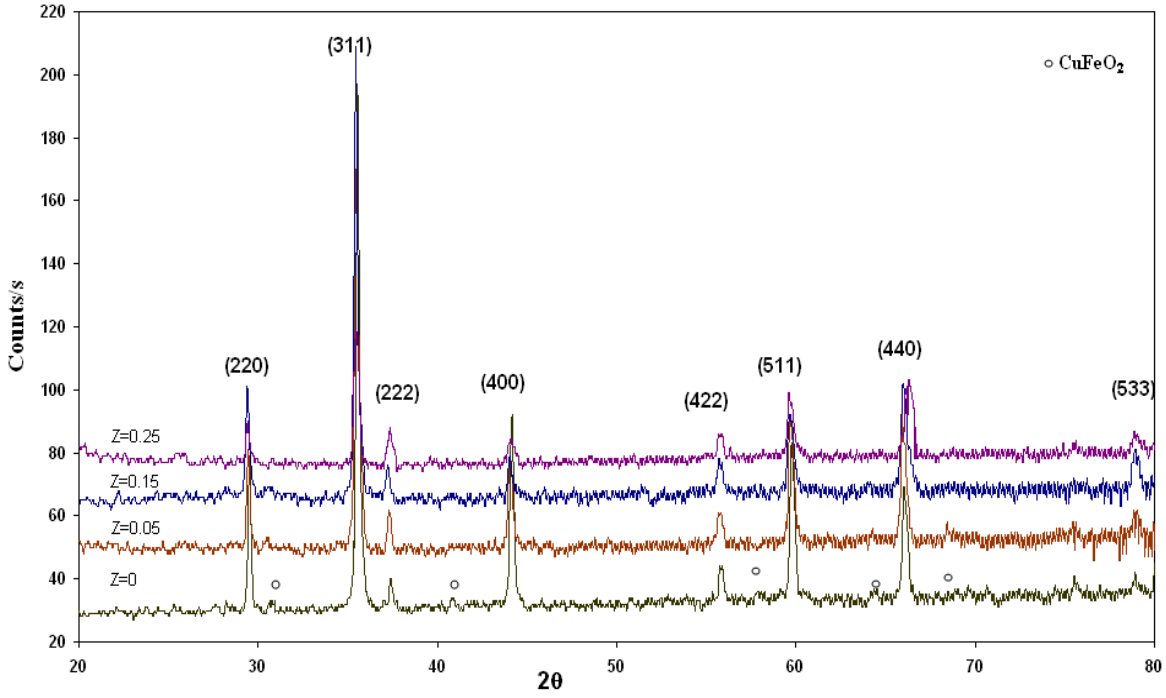

Fig. (2) X-ray diffraction pattern of $Cu_{0.7}Mg_{0.3}Bi_zFe_{2-z}O_4$; $0.0 \leq z \leq 0.25$

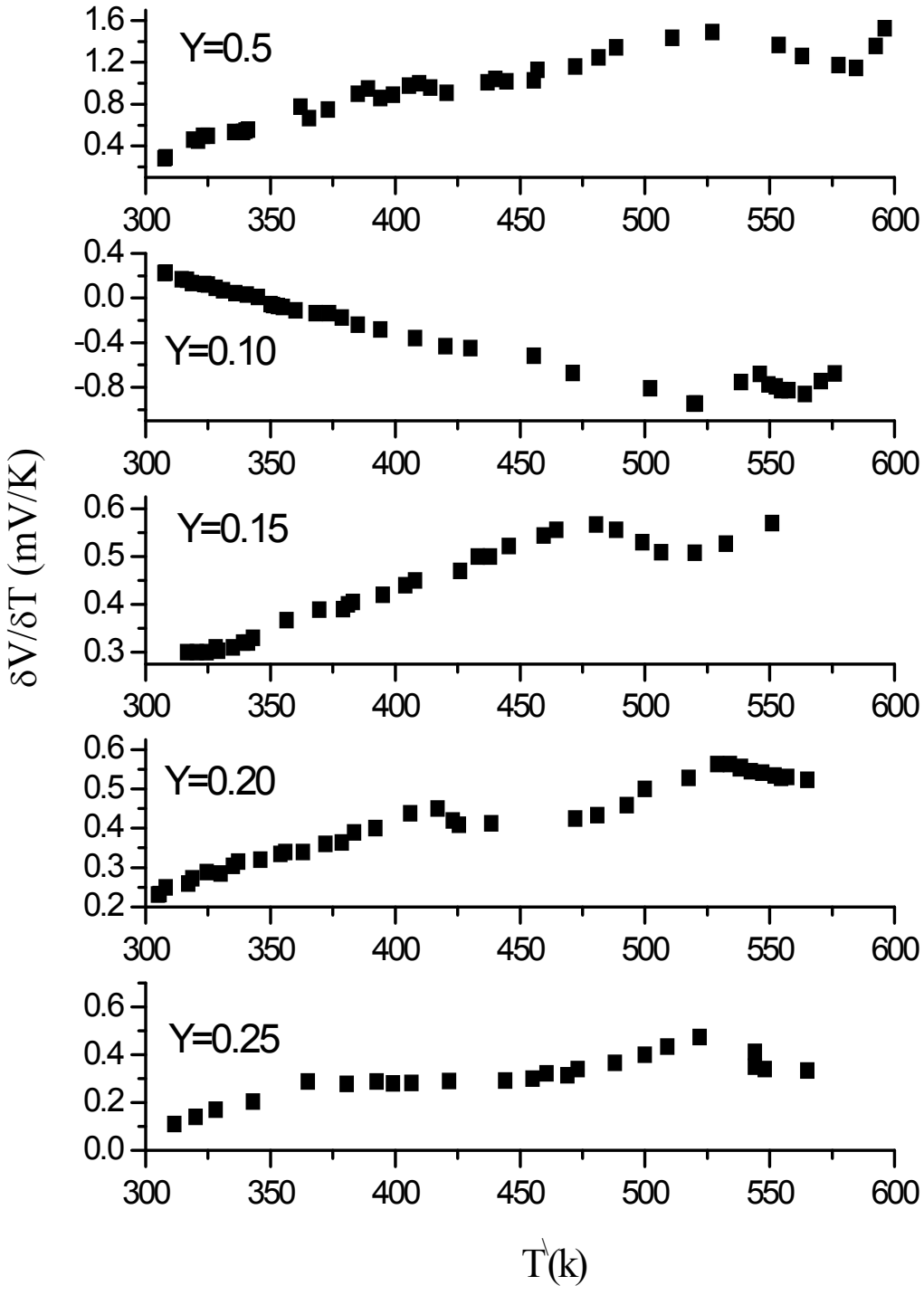

Fig. (3) Variation of Seebeck coefficient with the average of absolute temperature (T\) for $Cu_{0.7}Mg_{0.3}Sb_yFe_{2-y}O_4$; $0.05 \leq y \leq 0.25$

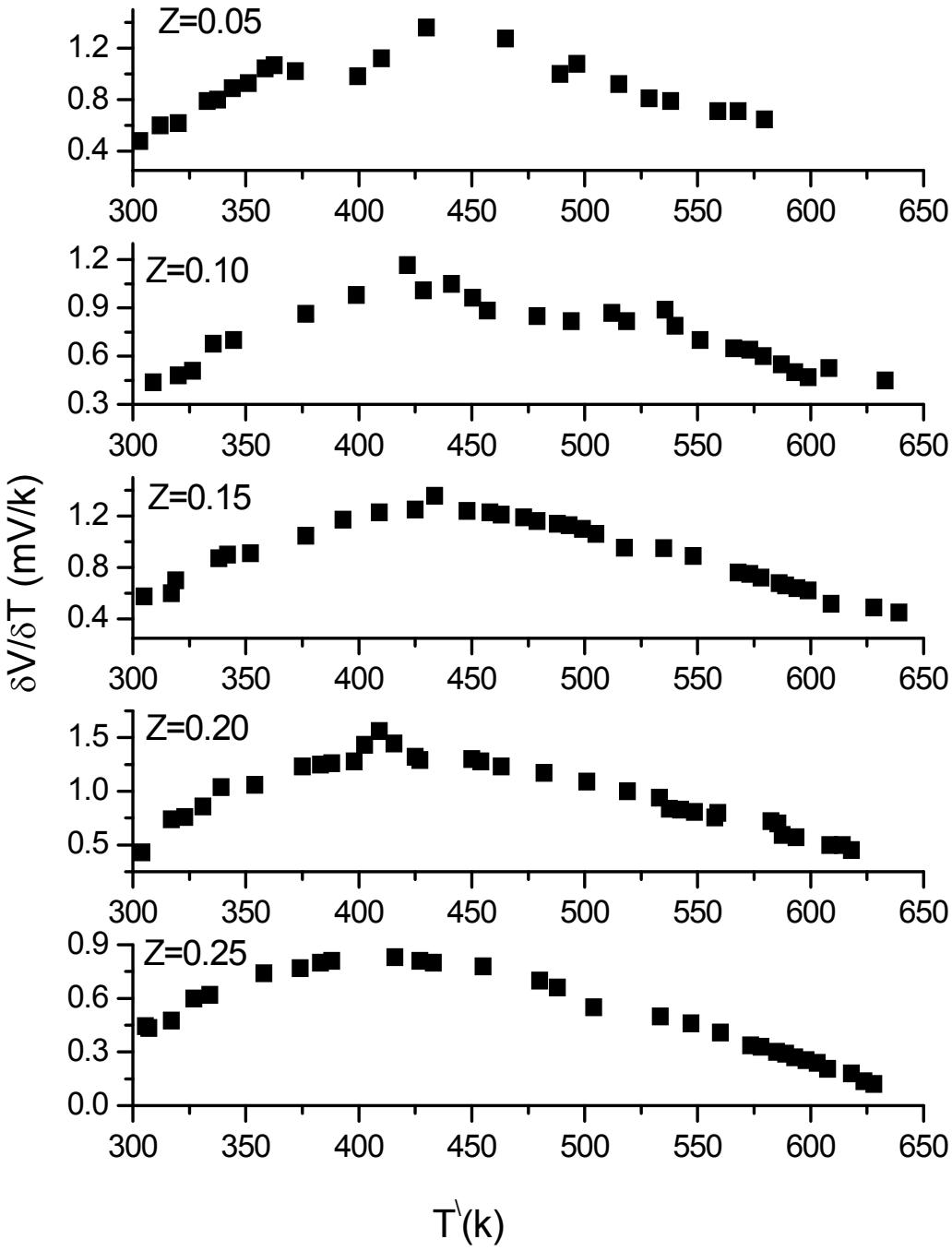

Fig. (4) Variation of Seebeck coefficient with the average of absolute temperature (T\) for $Cu_{0.7}Mg_{0.3}Bi_zFe_{2-z}O_4$; $0.0 \leq z \leq 0.25$

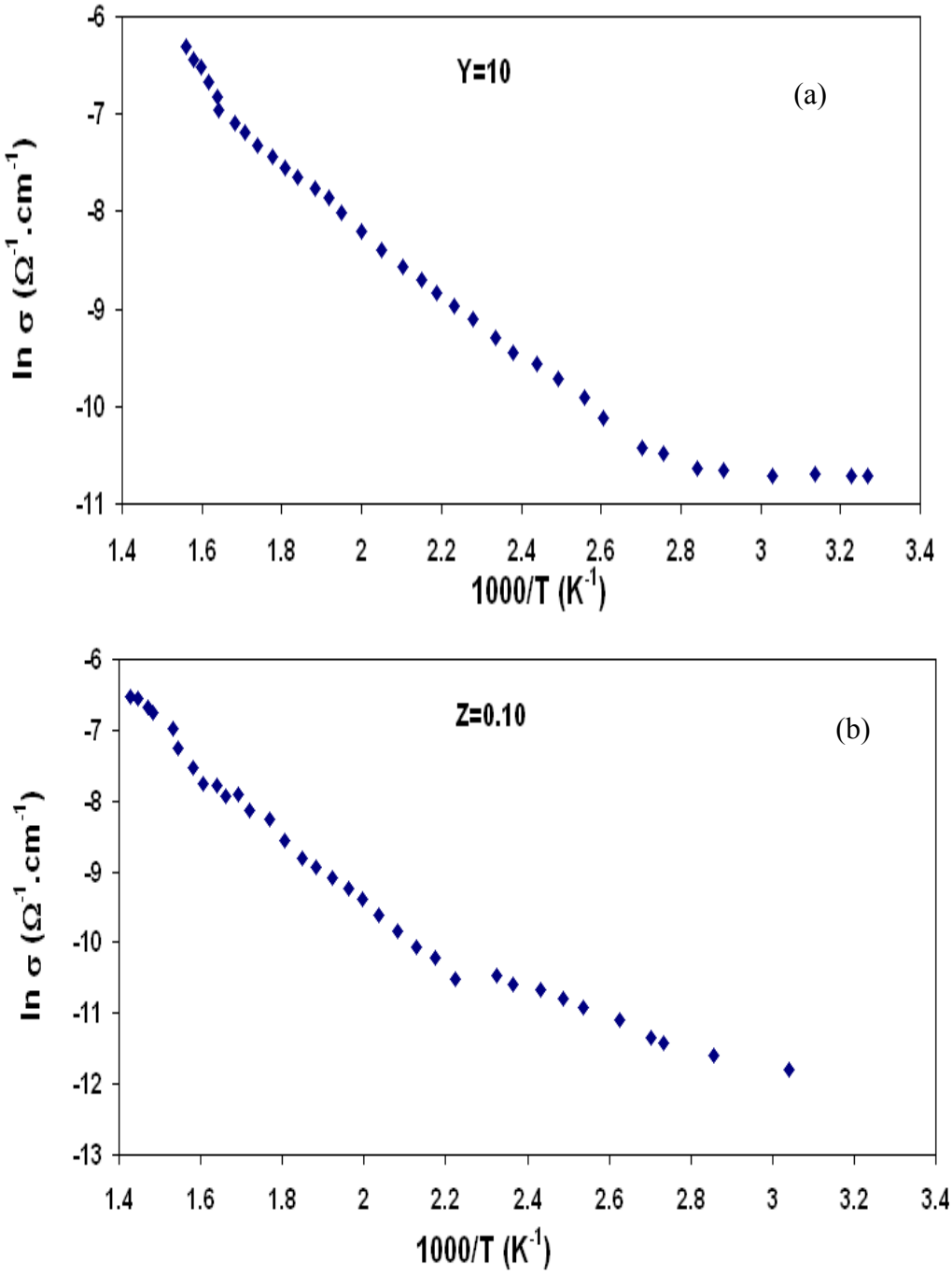

Fig. (6) Typical curve of ac electrical conductivity (ln) Vs (1000/T) K^{-1} for
(a) $Cu_{0.7}Mg_{0.3}Sb_yFe_{2-y}O_4$; $0.0 \leq y \leq 0.25$
(b) $Cu_{0.7}Mg_{0.3}Bi_zFe_{2-z}O_4$; $0.0 \leq z \leq 0.25$

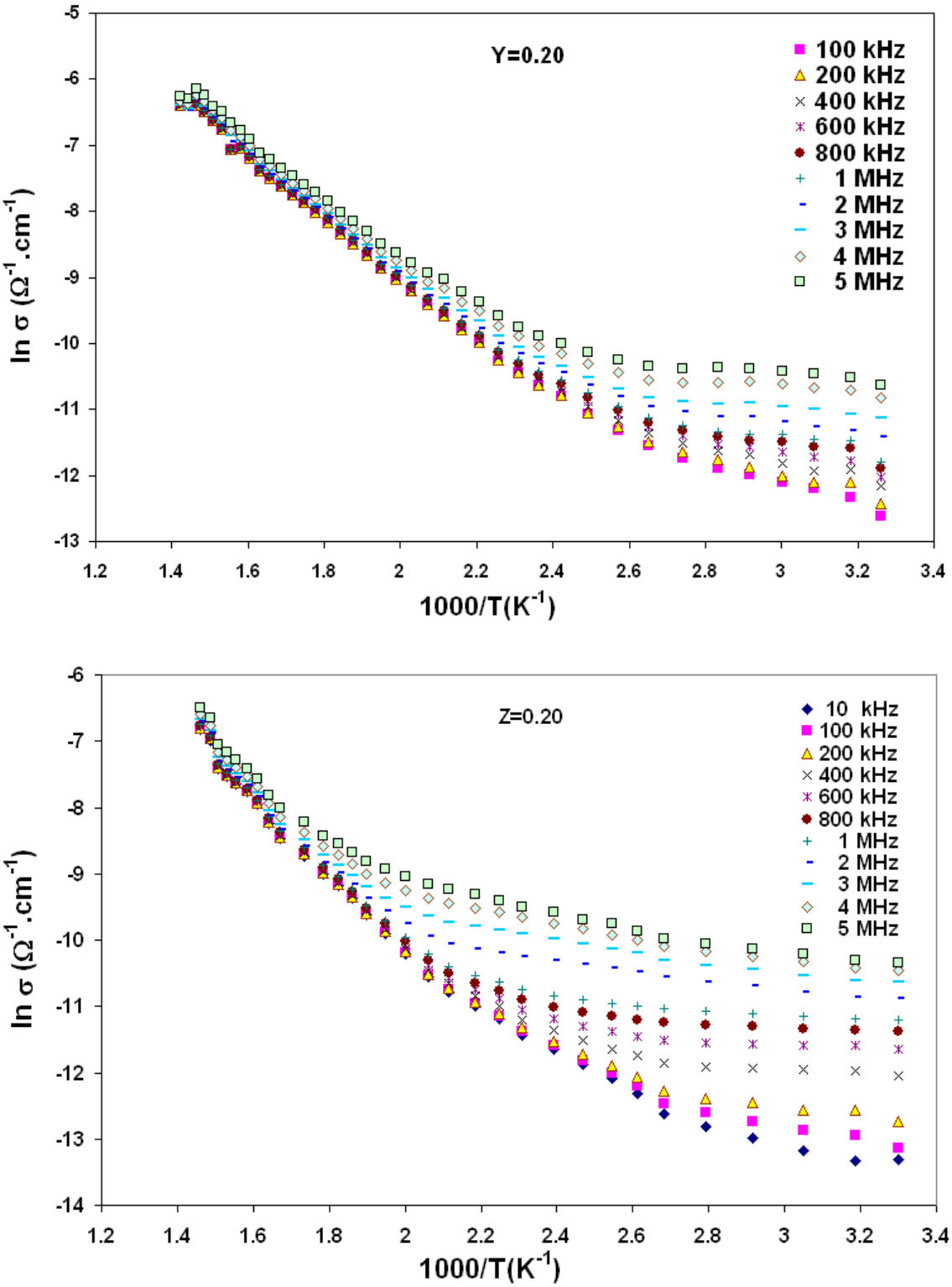

Fig. (6) Typical curve of ac electrical conductivity (ln σ) Vs (1000/T) K^{-1} for
(a) $Cu_{0.7}Mg_{0.3}Sb_yFe_{2-y}O_4$; $0.0 \leq y \leq 0.25$
(b) $Cu_{0.7}Mg_{0.3}Bi_zFe_{2-z}O_4$; $0.0 \leq z \leq 0.25$

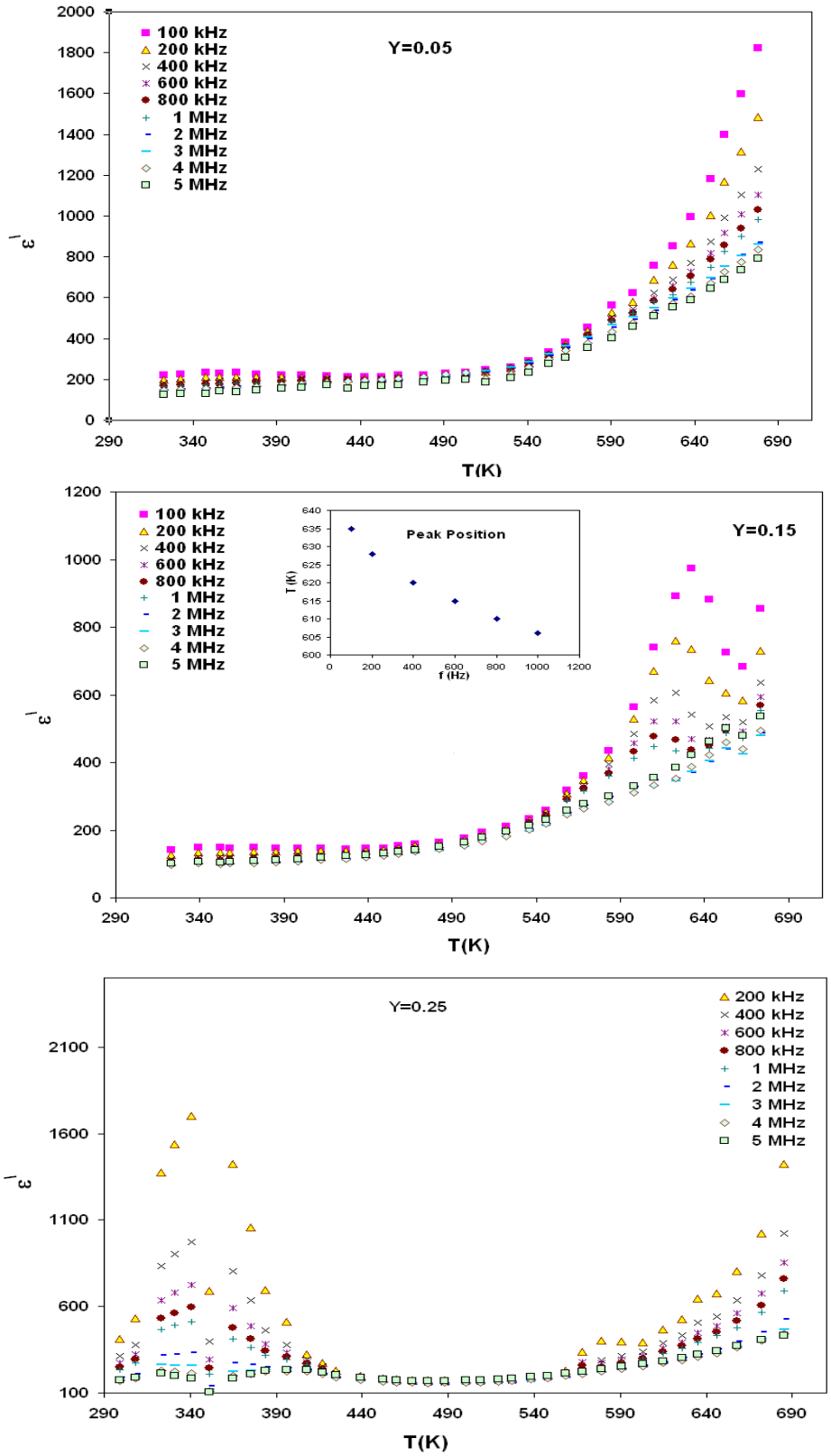

Fig. (7) Temperature dependence of dielectric constant (ε') at different frequencies of $Cu_{0.7}Mg_{0.3}Sb_yFe_{2-y}O_4$; $0.0 \leq y \leq 0.25$

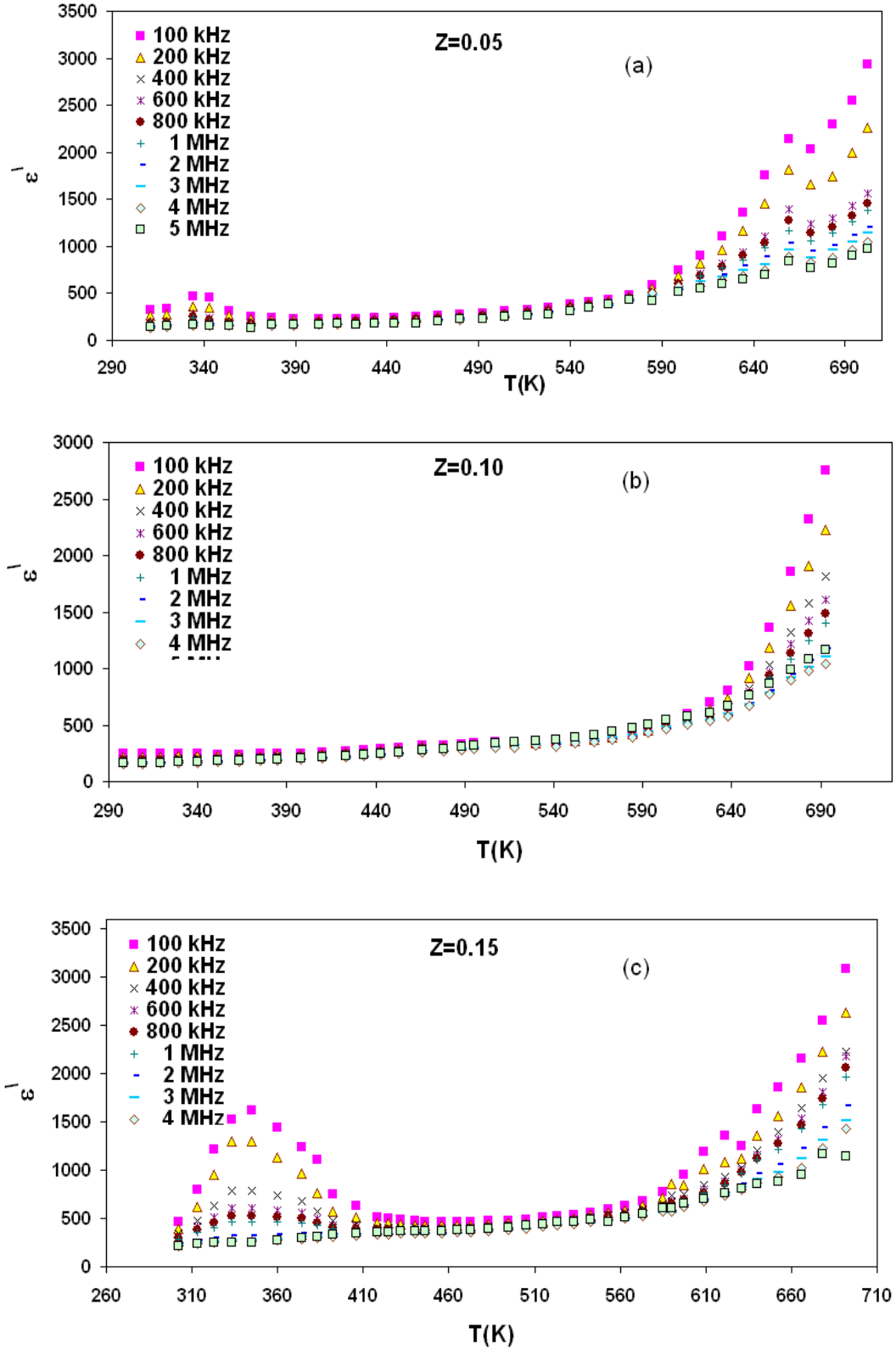

Fig.(8) Temperature dependence of dielectric constant (ε') at different frequencies of $Cu_{0.7}Mg_{0.3}Bi_zFe_{2-z}O_4$; $0.0 \leq z \leq 0.25$

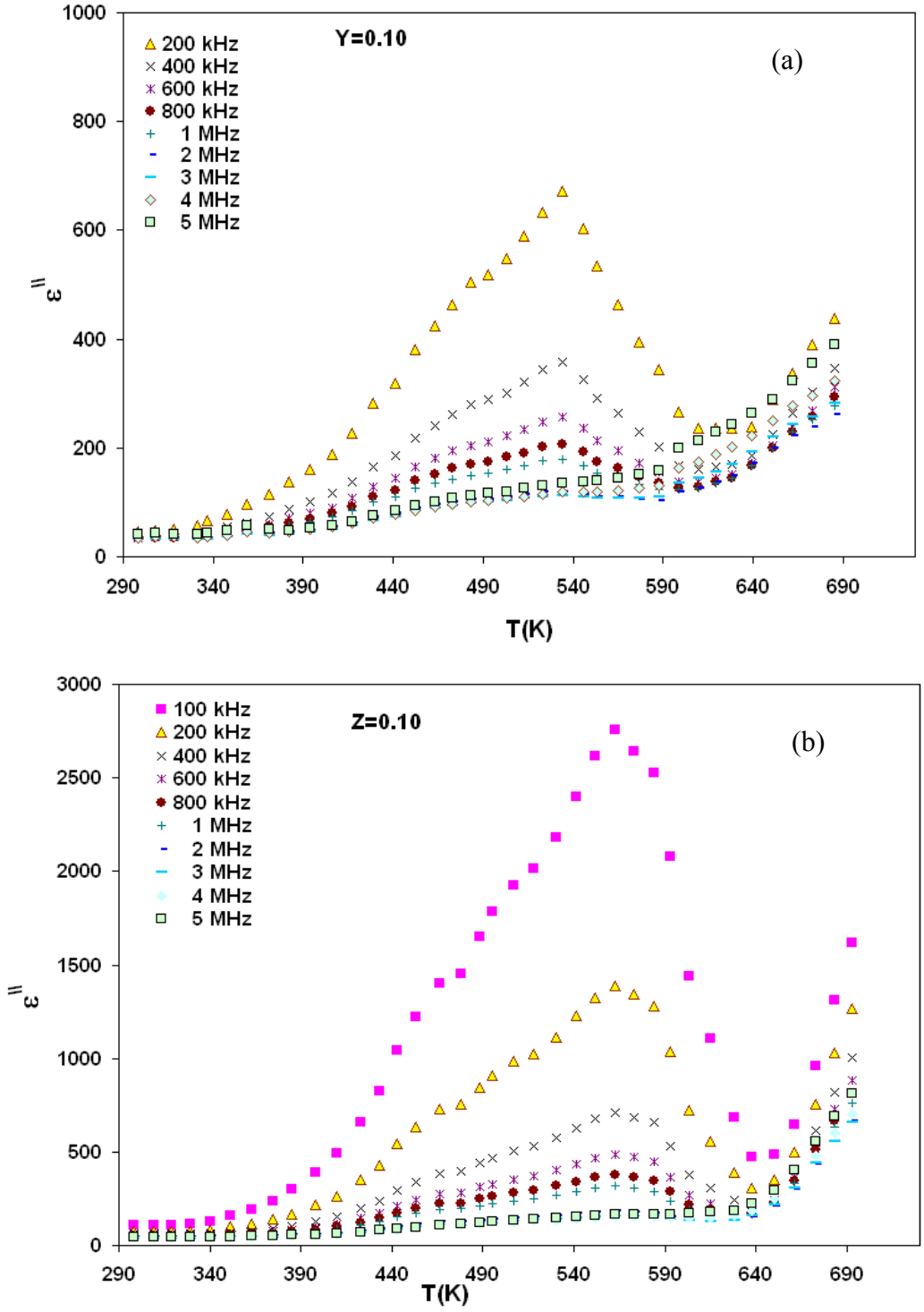

Fig. (9) Typical curve of temperature dependence of dielectric loss factor (ε'') at different frequencies of
(a) $Cu_{0.7}Mg_{0.3}Sb_yFe_{2-y}O_4$; $0.0 \leq y \leq 0.25$
(b) $Cu_{0.7}Mg_{0.3}Bi_zFe_{2-z}O_4$; $0.0 \leq z \leq 0.25$

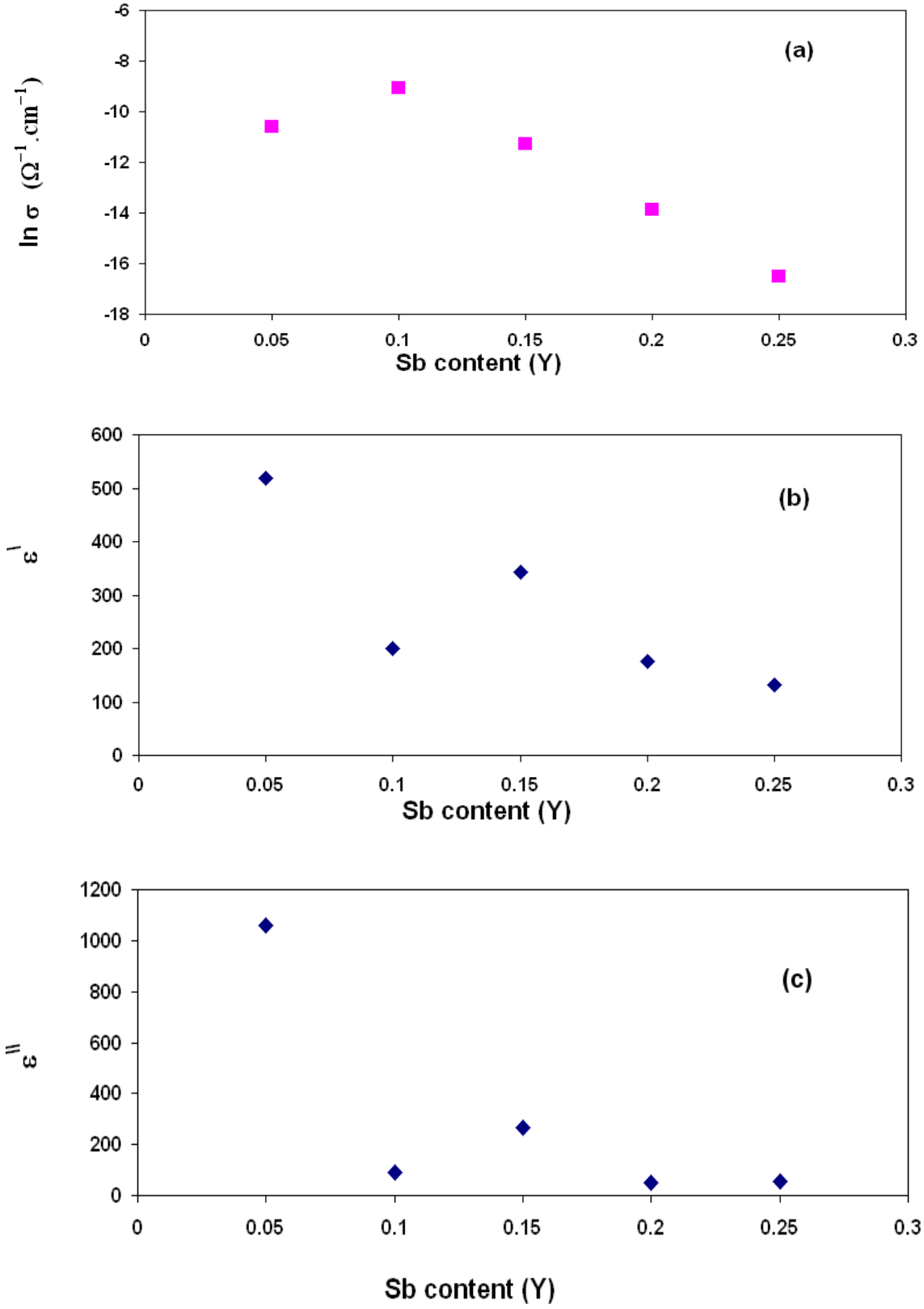

Fig. (10) The composition dependence of $Cu_{0.7}Mg_{0.3}Sb_yFe_{2-y}O_4$; $0.0 \leq y \leq 0.25$
(a)AC conductivity (b) Dielectric constant (ε') (c) Dielectric loss factor (ε'')

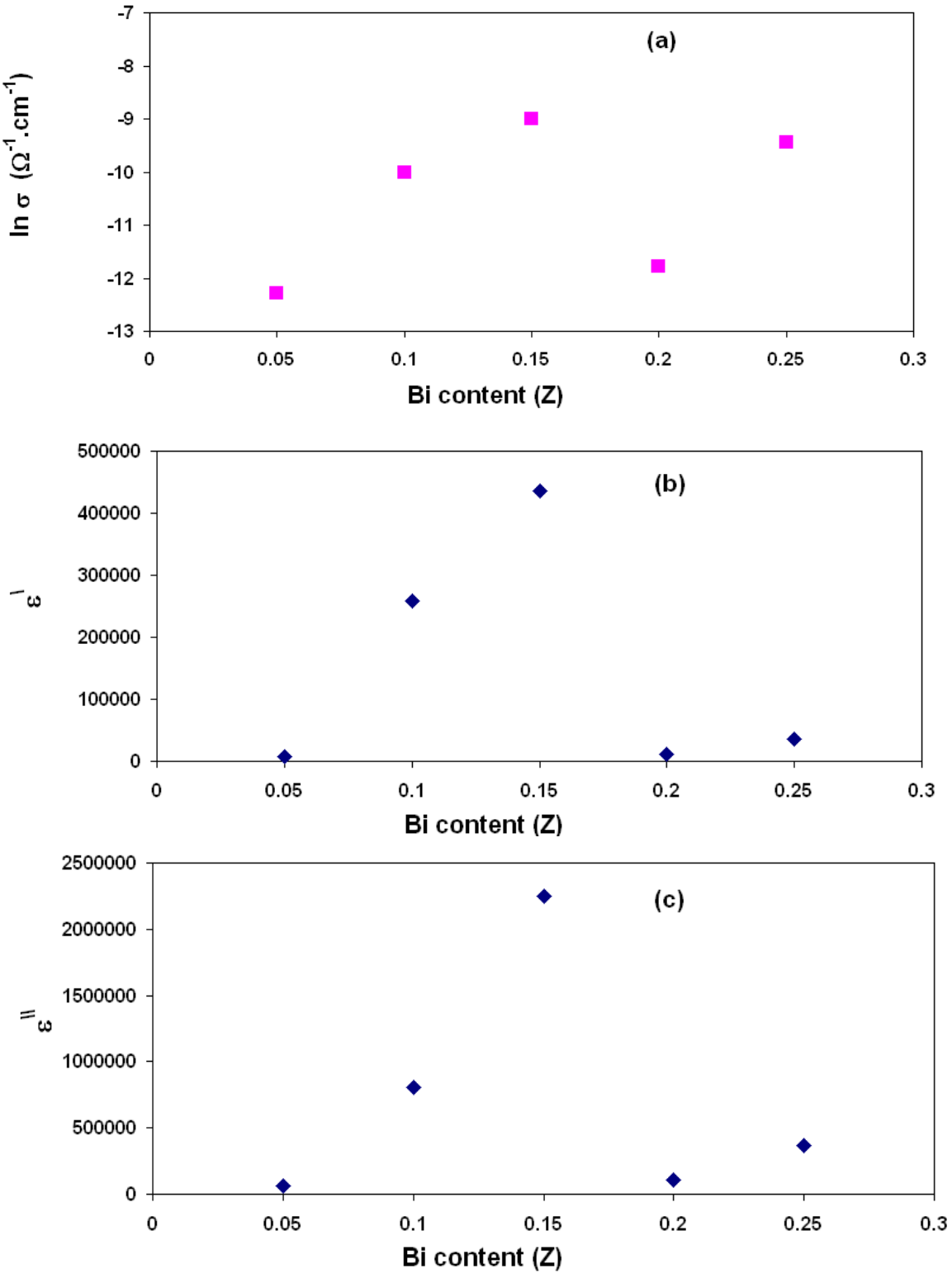

Fig. (11) The composition dependence of $Cu_{0.7}Mg_{0.3}Bi_zFe_{2-z}O_4$; $0.0 \leq z \leq 0.25$
(a)ac conductivity (b) Dielectric constant (ε') (c) Dielectric loss factor (ε'')

Conclusion

The composition $Cu_{0.7}Mg_{0.3}Sb_yFe_{2-y}O_4$ showed spinel structure with small secondary phase at $y \geq 0.15$, while the $Cu_{0.7}Mg_{0.3}Bi_zFe_{2-z}O_4$ showed single phase cubic spinel ferrites. The lattice parameter decreases with increasing both Sb^{3+} and Bi^{3+}.

All samples gives positive values of Seebeck coefficient which indicates the majority of charge carriers are holes (p-type). The ac conductivity deceases with increasing Sb^{3+} content, it increases with increasing Bi^{3+} content up to y=0.15 and then decreases. The deceases and increases is due to change the ratio of Fe^{2+}/Fe^{3+} and Cu^{2+}/Cu^{+1}.

Acknowledgments

The authors would like to express their appreciation to the cooperation of Khanjar institute For Scientific Development, and its president Mr. Khamees F. AlKhanjar for the financial and moral support for the completion of this research.

Corresponding author

A. Almuhamady

Materials Science Lab, Physics Department, Faculty of Science, Cairo University, Giza, Egypt

a.almuhamady@yahoo.com

References

[1] Toshiyuki Suzuki, Termitsu Tanaka, Kaoru Ikemizu," High density recording capability for advanced particulate media" J. Magn. Magn. Mater. **235** (2001) 159.

[2] T. Giannakopoulou, L. Kompotiatis, A. Kontogeorgakos, G. Kordas" Microwave behavior of ferrites prepared via sol–gel method" J. Magn. Magn. Mater. **246** (2002) 360.

[3] E. Olsen, J. Thonstad," Nickel ferrite as inert anodes in aluminium electrolysis" J. Appl. Electrochem. **29** (1999) 293.

[4] C.O. Augustin" Sintering behaviour of NiO-Fe_2O_3 composites" J. Mater. Sci Lett. **12** (1993) 1786.

[5] J. Kulikouski, A. Leśniewski " Properties of Ni-Zn ferrites for magnetic heads: Technical possibilities and limitations" J. Magn. Magn. Mater. **19** (1980) 117.

[6] E.E. Riches, in: J.G. Cook (Ed.)," Ferrites: A Review of Materials and Applications" Miles and Boons, London, 1972, p. 17.

[7] R. D. Shannon "Revised effective ionic radii and systematic studies of interatomic distances in halides and chalcogenides." Acta Crystallographica. **A32**, (1976) 751.

[8] D. Ravinder, "Thermoelectric Power and Electrical Resistivity of Cadmium-Substituted Manganese Ferrite," Materials Letters**, 44** (2003) 130.

[9] S.A. Mazen and A. Elfalaky "Thermoelectric power and electrical conductivity of Cu–Ti ferrite" J. Magn. Magn. Mater.**195** (1999) 148.

[10] Li-yuan Zhang, Chun-lei Liu, Xiao-qiang Yang and Qiang Han" Thermoelectric power and Hall effect of high-Tc superconductors in a two-component model" Physica B, **279,** (2000) 230.

[11] D. Ravinder, G. Ravi Kumar and Y.C. Venudhar" High-temperature thermoelectric power studies of copper substituted nickel ferrites" Journal of Alloys and Compounds, **363**(2004)6.

[12] P.V. Reddy, V.D. Reddy and D. Ravinder" Thermopower studies of lithium–zinc mixed ferrites" Phys. Stat. Sol.(a) **127** (1991) 439.

[13] N. Rezlescu and E. Rezlescu 'Dielectric properties of copper containing ferrites' Phys. Stat. Sol. (a) **23** (1974) 575.

[14] B. Kunar, G. Srivastava," Dispersion observed in electrical properties of titanium-substituted lithium ferrites' J. Appl. Phys. **75**, (1994) 6115.

[15] C. Koops," On the Dispersion of Resistivity and Dielectric Constant of Some Semiconductors at Audiofrequencies" Phys. Rev. **83** (1951) 121.

[16] P. Haberey and H. Wijn," Effect of temperature on the dielectric relaxation in polycrystalline ferrites" Phys. Stat. Sol. (b) **26**, (1968) 231.

[17] J.Smith and H.P.J.Wijn "Ferrites", John Wiley & Sons, Inc., New York, (1959)

[18] W.D. Kingery, H.K. Bowen and D.R. Uhlman" Introduction to Ceramics" 2nd ed., Ch. 18, Wiley, New York, (1976).

6/3/2012